Matter-wave interference in an axial triple-well optical dipole trap*

Zhou Qi(周 琦)[a)b)], Lu Jun-Fa(陆俊发)[b)], and Yin Jian-Ping(印建平)[a)†]

[a)] *State Key Laboratory of Precision Spectroscopy, Department of Physics, East China Normal University, Shanghai* 200062, *China*

[b)] *Department of Physics, East China Institute of Technology, Jiangxi Fuzhou* 344000, *China*

(Received 11 November 2009; revised manuscript received 8 February 2010)

This paper proposes a scheme of axial triple-well optical dipole trap by employing a simple optical system composed of a circular cosine grating and a lens. Three optical wells separated averagely by ∼37 μm were created when illuminating by a YAG laser with power 1 mW. These wells with average trapping depth ∼0.5 μK and volume ∼74 μm^3 are suitable to trap and manipulate an atomic Bose–Einstein condensation (BEC). Due to a controllable grating implemented by a spatial light modulator, an evolution between a triple-well trap and a single-well one is achievable by adjusting the height of potential barrier between adjacent wells. Based on this novel triple-well potentials, the loading and splitting of BEC, as well as the interference between three freely expanding BECs, are also numerically stimulated within the framework of mean-field treatment. By fitting three cosine functions with three Gaussian envelopes to interference fringe, the information of relative phases among three condensates is extracted.

Keywords: triple-well optical trap, matter-wave interference, spatial light modulator
PACC: 3280P, 0530, 4225F

1. Introduction

In recent years, there is an interest-increasing research for the interference of matter wave,[1−6] which not only provides a direct evidence of coherence nature of matter, such as phase coherence,[7] fluctuation[8] and long-range order[2] of a cold condensate, but also offers a powerful tool for demonstrating properties of atoms or molecules[9] and realizing exquisite precision measurement of fundamental constants.[10−12] Many flexible systems, including optical microtraps generated by focused red-detuned laser light and acousto-optical modulator,[4] atom chip consisted of microfabricated current-carrying wires,[6,13−15] and microfabricated optical elements,[16,17] have been proposed theoretically or experimentally to construct various confined-atom interferometers. All of these devices rely on a controllable double-well system to realize atom–atom interactions, controlled splitting and recombination of atomic wave packets.

Comparing with interference of two-component condensates, less attention was paid to three- or multi-component ones due to more complex nonlinearity in physical mechanism and more compound structure in interference pattern. However, it can bring us more richer dynamics and applications. For example, a two-component interferometer has been used to sense electric and magnetic fields, as well as inertial and acceleration field,[11] while a three-component one is able to measure either these quantities or its gradient. To obtain such a system of multiple trapping sites, programmable diffractive optical devices are considered as candidates. Complex intensity profiles can be easily generated in Fourier plane by writing corresponding holograms on spatial light modulator(SLM). Currently, the interframe artifacts are also alleviated, even avoided, with the application of high-speed ferroelectric SLM[18,19] and make dynamic manipulation of atoms possible. A common drawback of these devices is that the generated multiple optical trapping sites are limited to a two-dimensional plane normal to optical axis. The time-sharing techniques,[20] which periodically add a stream of lens functions to holograms, have been developed to extend optical traps in three dimensions, but the price must be paid to reduce the refreshed rate for trapping sites, which will result in undesirable diffusion of atoms and make variation

*Project supported by the National Natural Science Foundation of China (Grant Nos. 10434060, 10674047 and 10804031), the National Key Basic Research and Development Program of China (Grant No. 2006CB921604), the Program for Changjiang Scholar and Innovative Research Team, and Shanghai Leading Academic Discipline Project (Grant No. B408), the Youth Foundation of Jiangxi Educational Committee (Grant No. GJJ09530), and the Scientific Research Foundation of ECIT (Grant No. DSH0417).
†Corresponding author. E-mail: jpyin@phy.ecnu.edu.cn
© 2010 Chinese Physical Society and IOP Publishing Ltd

of the potential rough in dynamic spatial control.

In this paper, we firstly propose a simple scheme to synchronously generate three optical trapping potentials in the direction of optical axis by using a circular cosine grating displayed in SLM, as described in Section 2. Based on this controllable triple-well potentials, we will perform a numerically stimulation for loading and splitting of Bose–Einstein condensations(BECs), as well as the interference between three freely expanding BECs, and main results are given in Section 3. Finally, a conclusion will be given in Section 4.

2. Axial triple-well optical dipole trap

The basic principle of our scheme to generate an axial controllable triple-well optical dipole trap is illustrated in Fig. 1. After shielded by a non-transparent diaphragm with a circular hole, whose radius a is 5 mm, the collimated YAG laser field with a wavelength of $\lambda = 1.06$ μm and a power of $P = 1$ mW perpendicularly passes through a circular cosine grating, and then is focused by a positive lens with a focal length of $f = 20$ mm. The complex transmission of grating is constructed according to following equation:

$$\begin{aligned} t &= t_0 + t_1 \cos(k\frac{\rho^2}{2z_0}) \\ &= t_0 + \frac{1}{2}t_1 \exp\left(-\mathrm{i}\,k\frac{\rho^2}{2z_0}\right) \\ &\quad + \frac{1}{2}t_1 \exp\left(+\mathrm{i}\,k\frac{\rho^2}{2z_0}\right), \end{aligned} \tag{1}$$

where t_0 and t_1 are the positive real constants and k indicates the wave number of incident light. A polar coordinate system has been applied in the grating plane, and the origin is superposed with the centre of the hole on the diaphragm plate. In fact, the cosine component can be regarded as an interference pattern between a plane wave and a divergent spherical wave assuming the SLM screen placed perpendicularly to the optic axis with a distance z_0 away from the centre of the spherical wave. After diffraction by this grating, the wave front of incident light is divided into a plane component and another two spherical component with two source points located at $\pm z_0$, respectively. When these three diffracted waves pass through a positive lens, three bright spots, i.e. an axial triple-well optical dipole trap with a red detuning, will be generated before, after and at the focal point of the lens. A quadrupole and Ioffe configuration (QUIC) trap consisted of two identical quadrupole coils and one Ioffe coil is used to prepare BEC by using radio frequency evaporative cooling.[21] The trapping centre of QUIC trap is overlapped with the focal point of lens to load efficiently cold atoms from a QUIC magnetic trap to an axial triple-well optical one.

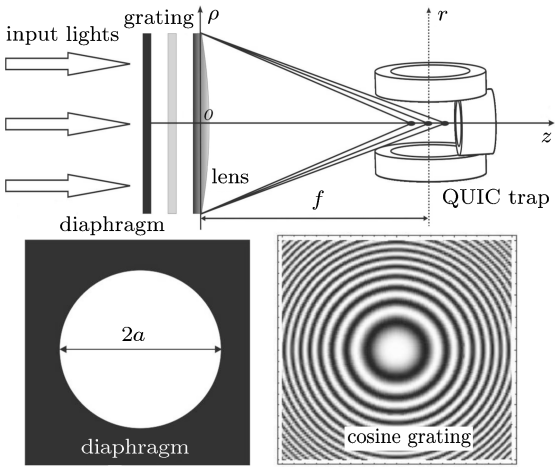


Fig. 1. Schematic of a tripe-well optical dipole trap for neutral atoms formed by a circular cosine grating and a lens, as described in the text.

A computer-driven transmission type SLM is used here to behave as a diffraction grating. Thus, the cosine patterns can be rapidly written in real time by control signals, which is especially significant to implement evolution between triple-well trap and single-well one. In our case, when $t_0 \geq t_1$, only amplitude modulation is needed, which is decided by $|t|$. However, an additional ring-shaped phase modulation should be applied to the area of $t_0 < t_1$ and the phase is alternated between zero and π according to $\mathrm{sgn}(t)$. Another approach is using additional algorithms, such as direct binary search,[22] to transform a mixed modulation diffraction grating to a pure phase modulation one.

When the separations between the diaphragm and grating, as well as the grating and lens are ignored, the complex amplitude and intensity distribution of light field in image space, in cylindrical coordinates, are given by

$$\begin{aligned} U(r,z) = \int_0^{2\pi}\int_0^{a} \Bigg\{ U_0 \Bigg[& t_0 \mathrm{e}^{\mathrm{i}\,k\left(\frac{\rho^2}{2z} - \frac{\rho^2}{2f} - \frac{\rho r\cos\theta}{z}\right)} \\ & + \frac{1}{2}t_1 \mathrm{e}^{\mathrm{i}\,k\left(\frac{\rho^2}{2z_0} + \frac{\rho^2}{2z} - \frac{\rho^2}{2f} - \frac{\rho r\cos\theta}{z}\right)} \\ & + \frac{1}{2}t_1 \mathrm{e}^{\mathrm{i}\,k\left(-\frac{\rho^2}{2z_0} + \frac{\rho^2}{2z} - \frac{\rho^2}{2f} - \frac{\rho r\cos\theta}{z}\right)} \Bigg] \Bigg\} \rho \mathrm{d}\rho \mathrm{d}\theta, \end{aligned}$$

$$I(r,z) \propto \frac{1}{\lambda^2 z^2} |U(r,z)|^2 . \quad (2)$$

In Eq. (2), an unessential phase factor is ignored, and U_0 is initial amplitude distribution of the incident light in diaphragm plane. Considering that the beam waist w_0 of the incident laser is sufficiently larger than the radius of the aperture so that the difference from the illuminations by using Gaussian beam and plane-wave one can be canceled, a plane wave approximation can be used to simplify our calculation. In order to make use of the most of output power, a suitable option is $w_0 = \sqrt{2}a$, which offers an average light intensity ($I_0 \propto |U_0|^2$) of ∼12.7 W/m^2 when the incident laser power tune up to 1 mW.

According to Eq. (2), we calculated the optical field distribution for $z_0 = 15000$ mm, $t_0 = 0.33$ and $t_1 = 0.5$, and the results are shown in Fig. 2. In this figure, the zero point of the z axis is chosen at the focal point of the lens. It is clear from Fig. 2 that there are three cigar-type traps, and the separated distance between two adjacent traps is 37.5 μm along the optical axis. To know the characteristics of the generated optical wells, 2D intensity contours in the yoz and xoy planes are also plotted. Though the volume of the middle well centred at the focal point is slightly larger than the two side, three wells have the same maximal intensity, height of barriers and aspect ratio, which are 9.3 MW/m^2, 3.6 MW/m^2 and 11:1 ($\Delta z_{1/e2} : \Delta r_{1/e2}$), respectively. For ^{87}Rb atoms with D_2-line transition $5S_{1/2}(F = 2) \leftrightarrow 5P_{2/3}$, trapping depth of each potential well and their average $1/e^2$ volume are about 526 nK and 74 μm^3, which are suitable to trap and manipulate atomic BEC.[23,24]

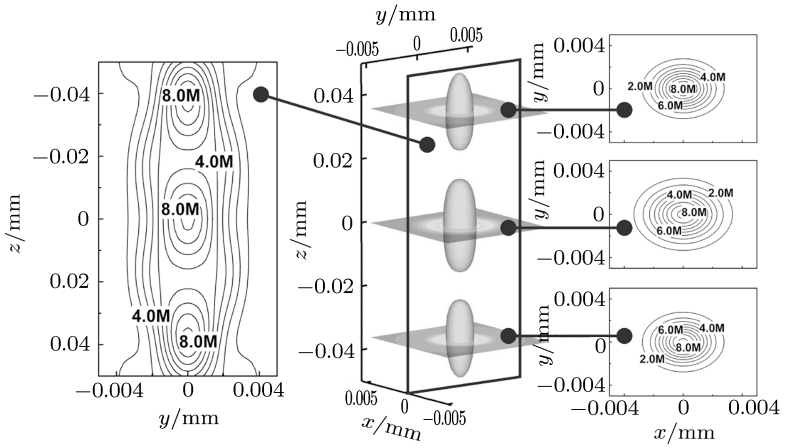


Fig. 2. The central diagram is three-dimensional (3D) intensity distribution of generated tripe-well optical dipole trap. 3D cigar-type isopotential surfaces represent points of a constant optical intensity with $I = 6$ MW/m^2. The left are 2D intensity contours of three optical wells in the yoz plane and the right in the planes parallel to the xoy plane, here the centres of three wells are located at $z = -37.5$, 0.0 and 37.5 μm, respectively.

By adjusting the z_0 and t_0 of the cosine grating, we are able to control either the separation or the height of barrier between two adjacent wells, and a tripe-well trap can evolve into a quasi-single-well trap, which still contains two small barriers. This process is shown in Fig. 3. With simultaneously and linearly increasing z_0 (from 15000 mm to 16600 mm) and t_0 (from 0.33 to 0.35), trap centres of three wells will shift close to each others, and the barriers fall down. In particular, when $z_0 = 16600$ mm and $t_0 = 0.35$, these barriers with about 10–20 nK height are so small than the intrinsic energy of a BEC that it can be used to load BEC from QUIC trap and keep its coherence unchanged.

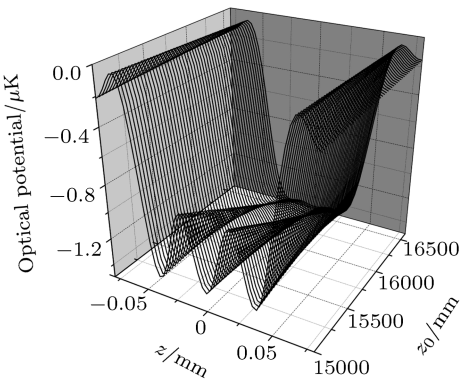


Fig. 3. The evolution of our optical dipole trap from a tripe-well trap to a quasi-single-well one for simultaneously and linearly adjusting z_0 (from 15000 mm to 16600 mm) and t_0 (from 0.33 to 0.35). The trapping potentials are calculated for ^{87}Rb atom with D_2-line transition $5S_{1/2}(F = 2) \leftrightarrow 5P_{2/3}$.

3. Matter-wave interference

3.1. Mean-field model

Now, we will perform a numerical simulation of interference formed by combining three clouds of atomic BEC originating from a single condensate. Our calculations are based on the time-dependent mean-field Gross–Pitaevskii equation with an axial symmetry[25]

$$\left[-\mathrm{i}\,\hbar\frac{\partial}{\partial t}-\frac{\hbar^2}{2m}\left(\frac{\partial^2}{\partial r^2}+\frac{1}{r}\frac{\partial}{\partial r}+\frac{\partial^2}{\partial z^2}\right)+V\left(r,z\right)+gN\left|\psi\left(r,z;t\right)\right|^2\right]\psi\left(r,z;t\right)=0, \tag{3}$$

where $\psi\ (r,z;t)$ is the time-dependent BEC wave function, m is the mass of atom, N is the number of atoms in the condensate, and $g=4\pi\hbar^2a/m$ is the strength of interatomic interaction defined in terms of the s-wave scattering length a. The combined potential of harmonic magnetic trap (QUIC trap) and our optical trap are given by $V(r,z)=(1/2)m\omega^2(r^2+v^2z^2)+V_{\mathrm{opt}}$, where ω and v are the angular frequency in the radial direction and the aspect ratio of magnetic trap, respectively, and V_{opt} is the optical potential of our optical trap, as shown in Fig. 3. After transforming to dimensionless units by $r'=\sqrt{2}r/l, z'=\sqrt{2}z/l$, $\tau=t\omega$, $l=\sqrt{\hbar/(m\omega)}$, and $\psi\left(r',z',\tau\right)=\sqrt{4\pi l^3}\psi\left(r,z,t\right)$, we rewrite Eq. (3) as

$$\left[-\frac{\partial}{\partial\tau}-\frac{\partial^2}{\partial r'^2}-\frac{1}{r'}\frac{\partial}{\partial r'}-\frac{\partial^2}{\partial z'^2}+\frac{1}{4}\left(r'^2+v^2z'^2\right)+\frac{V_{\mathrm{opt}}\left(r',z'\right)}{\hbar\omega}+N'\left|\psi\left(r',z',\tau\right)\right|^2\right]\psi\left(r',z',\tau\right)=0, \tag{4}$$

where $N'=aN/l$. The normalization condition of the reduced wave function $\psi\left(r',z',\tau\right)$ will be

$$\int_{-\infty}^{\infty}\mathrm{d}z'\int_{0}^{\infty}\left|\psi\left(r',z',\tau\right)\right|^2r'\mathrm{d}r'=4\sqrt{2}.$$

Equations (3) and (4) are the classical nonlinear Schrodinger equations (NLSE), which are generally known to be difficult to solve. We numerically solve this NLSE by adopting a split-step time-iteration method with the Crank–Nicholson discretization scheme as described in Refs. [26] and [27]. The full Hamiltonian can be conveniently decomposed as three parts to follows:

$$\begin{aligned}
&H=H_1+H_2+H_3,\\
&H_1=\frac{1}{4}\left(r'^2+v^2z'^2+\frac{V_{\mathrm{opt}}}{\hbar\omega}+N'\left|\psi\left(r',z',t\right)\right|^2\right),\\
&H_2=-\frac{\partial^2}{\partial r'^2}-\frac{1}{r'}\frac{\partial}{\partial r'},\\
&H_3=-\frac{\partial^2}{\partial z'^2},
\end{aligned} \tag{5}$$

where the first part contains the linear and nonlinear terms, the second one contains the r'-dependent derivative terms, and the final one contains the z'-dependent derivative terms. Discretizing Eq. (5) in both the spatial and temporal directions with a space interval of $\Delta r'=\Delta z'=0.1$ and a time interval of $\Delta\tau=0.001$, we can obtain the wave function in arbitrary time by time-iterative method once initial wave function is known.

3.2. Numerical results

In our numerical experiment, a BEC with $N=2\times10^5$ spin-polarised ^{87}Rb atoms in the hyperfine state $F=2$, $m_{\mathrm{f}}=2$ is firstly prepared in the QUIC trap, and then loaded them into our quasi-single-well optical trap. For numerical simulation, we start the time iteration with the known harmonic oscillator solution of the NLSE without the nonlinear term, i.e., $N'=0$ and $\psi\left(r',z'\right)=A\exp[-(r'^2+vz'^2)/4]$, where A is a normalization constant. The parameters of magnetic trapping potential are chosen as $\omega=240\times2\pi$ Hz and $v=0.316$. The optical potential created by our proposed scheme with $z_0=16600$ mm and $t_0=0.35$ is superposed with the magnetic trap, and calculated by numerical integration of Eq. (2). The harmonic oscillator length is $l=\sqrt{\hbar/(m\omega)}=0.6966$ μm for the mass $m=1.44\times10^{-25}$ kg of ^{87}Rb, which leads to a dimensionless length $l/\sqrt{2}=0.4926$ μm and a time unit $\omega^{-1}=0.66$ ms, respectively. For a repulsive interaction, the natural scattering length of ^{87}Rb is $a=5.82$ nm corresponding to $N'=1670.97$ and can be tuned by using a magnetic field due to the effect of Feshbach resonance. In order to lighten the burden of our numerical simulation and obtain insights on the underlying physics, N' will be set as 100 (correspond-

ing $a = 0.3483$ nm) in followed calculation.

During time iteration, we slowly and linearly increase nonlinearity N' from 0 to 100 and the power P of trap laser from 0 to 1 mW in 10^6 time steps $\Delta\tau$. After subsequently iterated 5×10^5 times without changing any parameter, the wave function in the combined potential is obtained. The corresponding probability $|\psi(r', z', t)|^2$ of the bound BEC, which is a typical cigar-shaped condensate with aspect ratio 1:10, is shown in Fig. 4(a).

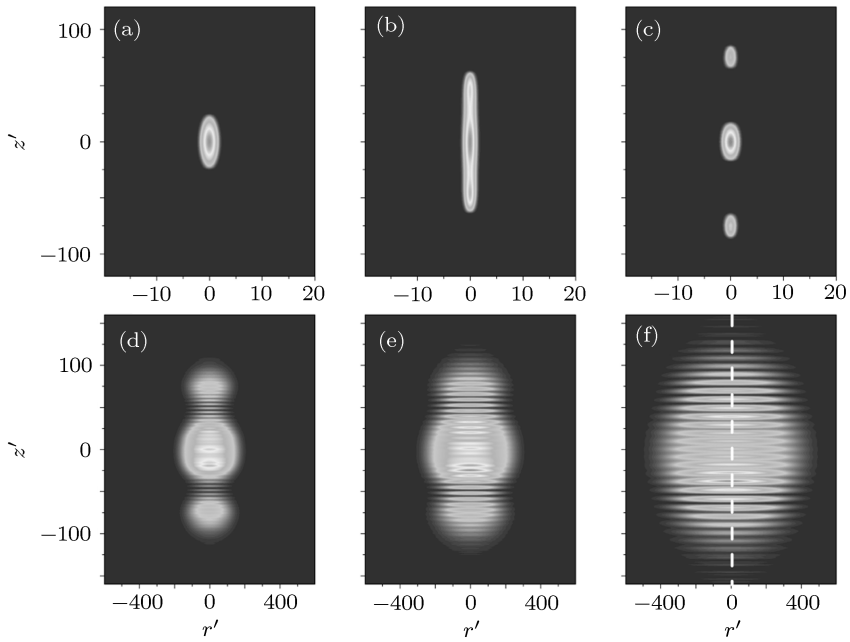


Fig. 4. The simulation of the loading, splitting and interfering formed by combining three clouds of atomic BEC. (a) The gray plot of the dimensionless wave function in combined magnetic and optical potentials. (b) The wave function after removing the magnetic potential. The condensate is completely loaded into the optical potential. (c) The splitted BECs after changing the parameters of the grating over 10^6 time steps and holding for another 5×10^5 time steps. The time evolution of the interference pattern after removing optical potential ($\tau = 0$) are shown in (d), (e) and (f) for the time-of-flight expansion of $\tau = 20$, $\tau = 30$ and $\tau = 50$, respectively.

Then, the magnetic potential is gradually closed down during another 10^6 time steps. The loading process is completed after holding atomic cloud for 5×10^5 times to permit the condensate atoms to tunnel through two narrow potential barriers in our quasi-single-well trap and obtain a stable wave function, which is exhibited in Fig.4 (b). By slowly and linearly changing the parameters of the grating over 10^6 time steps, we change adiabatically the optical potentials and transform a quasi-single-well trap into a tripe-well one, thereby dynamically splitting a BEC into three ones. The gray plot of probability of wave function after holding for another 5×10^5 time steps is shown in Fig.4(c). This figure clearly shows the formation of three bright structures in our tripe-well trap. The ratio of numbers of atoms trapped in three wells is about 0.14: 0.76: 0.12, which are calculated by integrating the wave function.

The simulation of interference among three condensates is performed by suddenly releasing these condensates from the optical traps. As a result, the atomic clouds ballistically expanded in free space and overlapped, and then an obvious interference pattern is produced due to phase coherence. In Figs. 4(d)–4(f), we show the interference patterns formed after the time-of-flight expansions of 20 (d), 30 (e) and 50 (f) time units, respectively. When the time of expansion is short, the interference patterns are formed by overlapping of two neighbouring condensates, which present in the segregated areas of three condensates. The fringe periods are 2.3 ($\tau = 20$) and 3.2 ($\tau = 30$) μm and increase with progressing expansion. Because of the repulsive interaction, they differ from the estimated values 1.6 ($\tau = 20$) and 2.4 ($\tau = 30$) μm by de Broglie wavelength associated with the relative motion of atoms $\lambda = 2h\tau/md$, which is an approximation of a non-interacting gas expanding from two point sources with a separation d. We also

notice that a slight fluctuation in wave function arises in the central condensate, which denotes the excited modes perhaps induced by numerical error in calculation of optical potential or quasi-continuous variation of the potentials in the process of splitting. In order to simulate the behaviour of SLM, we can only change its diffractive patterns from one value to another with a certain refreshed rate.

With a larger expansion time, each condensate grows large enough so that an interference pattern with all of three condensates is formed in the centre, see Fig. 4(f). Figure 5 also shows the axial probability density profiles along the dashed line in Fig. 4(f), which contains three sets of fringes respectively derived from each pair of condensates.

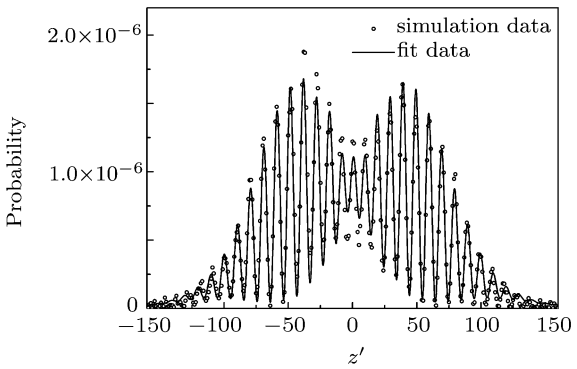


Fig. 5. The axial probability density profiles along the dashed line in Fig. 4(f). The hollow dots are the simulated data and the solid line is the fitted curve by three cosine functions with three Gaussian envelopes.

Our simulation data are plotted by hollow dots. We also fit three cosine functions with three Gaussian envelopes to these data in order to extract the information of relative phases among three condensates. Considering a quadratic phase profile for each condensate,[28] we have $\psi(z,t) = \sqrt{n_{\pm,0}}\exp\left\{\mathrm{i}\left[(m/2\hbar t)(z-d_{\pm,0})^2+\varphi_{\pm,0}\right]\right\}$, where the subscripts $\pm$, 0 denote each condensate with positive, negative and zero central position respectively, $n_{\pm,0}$ are Gaussian-type densities, $\varphi_{\pm,0}$ are the initial phases, $d_{\pm,0}$ are the central positions of condensates and we assume $d_{\pm} = \pm d$, $d_0 = 0$. So the total density profile can be expressed as

$$\begin{aligned} n(z,t) = {} & n_+ + n_- + n_0 \\ & +2\sqrt{n_0 n_+}\cos\left[\frac{md}{\hbar t}\left(z-\frac{d}{2}\right)+\Delta\varphi_1\right] \\ & +2\sqrt{n_0 n_-}\cos\left[\frac{md}{\hbar t}\left(z+\frac{d}{2}\right)+\Delta\varphi_2\right] \\ & +2\sqrt{n_+ n_-}\cos\left(\frac{2md}{\hbar t}z+\Delta\varphi_1+\Delta\varphi_2\right), \end{aligned} \quad (6)$$

where $\Delta\varphi_1 = \varphi_0 - \varphi_+$, $\Delta\varphi_2 = \varphi_- - \varphi_0$. The solid fitting curve is also plotted in Fig. 5, and the estimated relative phases, $\Delta\varphi_1 = 145.1^\circ$ and $\Delta\varphi_2 = -198.0^\circ$, are in rough agreement with the numerical value directly calculated from complex wave function, which are $\Delta\varphi_1 = 175.4^\circ$ and $\Delta\varphi_2 = -163.6^\circ$, respectively.

Moreover, we also perform a series of simulations of interference with different well separations. The relationship between the centres of condensates and the centres of our optical wells during the entire splitting process is shown in Fig. 6. The splitting process can be terminated at any time t_s, which corresponds to an expected separation, and the time-of-flight expansion is subsequently performed. After the loading process, the chemical potential of the condensates in the bottom of quasi-single-well optical trap is estimated as about 100 nK. For a small separation, the potential barriers are lower than the energy of the condensates so that the phases of condensates keep identical by tunnel coupling. So, the resulting image did not exhibit interference fringes except for two peaks arising in the positions of potential barriers. Once the height of barriers exceeds the chemical potential, the three condensates are isolated completely, and obvious interference patterns are presented. With the increase of separation, the interference fringe becomes denser.

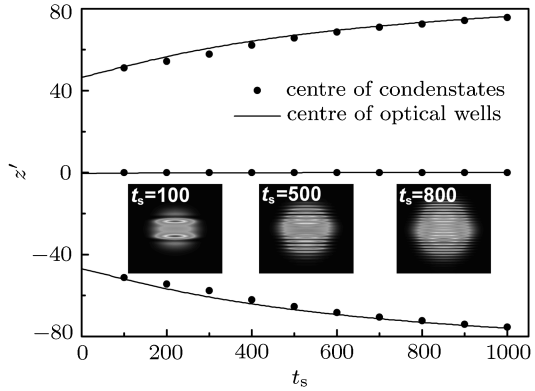


Fig. 6. The relationship between the centres of condensates and the centres of our optical wells during the entire splitting process. t_s is the splitting time. The insert plots show interference pattern released from different splitting time (left: $t_\mathrm{s} = 100$; centre: $t_\mathrm{s} = 500$, right: $t_\mathrm{s} = 800$), and formed by the time-of-flight expansion of 50 time units.

4. Conclusion

In conclusion, we have proposed a novel scheme to form a controllable axial triple-well optical dipole trap by using a circular cosine grating and a lens. Due to an adjustable height of potential barriers, a continual evolution between triple-well trap and single-well one

is achievable and a numerical stimulation of interference has also been discussed. Our studies show that the proposed scheme is suitable to trap and coherently manipulate an atomic BEC, and can be used to form a novel precision atom interferometer with three BECs. Some advantages of our proposed scheme are concluded as follows: (i) All operations of manipulating atomic wave packet can be finished in a simple way of controlling the cosine pattern in real time without any extra auxiliary system, e.g., optical Brag pulses or radio frequency field which is used to split and combine the condensates in atom interferometers based on optical pulses of light[12] or atomic chip.[6] Compact structure is also benefited to reduce the number of noise sources. (ii) the arrangement of axial splitting will result in a longer de Broglie wave-length, because the expansion of condensates in the axial direction is slower than one in the radial direction. The calculated fringe period of interference pattern is about 3 μm, corresponding to matter wavelength of 6 μm. It equals sources of moving atoms with a kinetic energy of 3 nK, which is much smaller than the single-photon recoil energy of 180 nK (780 nm) or the mean-field energy of Bose condensates in our trap (100 nK). So, the degree of precision based on our design is expected to enhance 1–2 orders in comparison with the interferometer with optical pulses of light or radial splitting ones. (iii) The interference of three condensates takes on a symmetric three-path configuration, which have been proved that the error from vibrational phase shifts and the effect of magnetic bias fields and gradients can be efficiently suppressed due to the symmetry.[12] Our future work will concentrate on whether the contrast oscillation presents in our regime, as that described in Ref. [12].

For further applications, arbitrary multiple traps in the optical axis are expected to be achieved conveniently by increasing the number of cosine functions. By adding these cosine patterns to the holograms used to create 2D intensity profiles, a 3D intensity profile will be generated. The trap can also be used to study some basic physics. For example new types of Josephson oscillations in a triple-well trap have been investigated theoretically,[29] which can be transmitted to self-trapping state by controlling the atomic interaction. A BEC in a three-well potential structure is expected to present a transistor-like behaviour[30] and switch effect,[31] in which the tunneling of atoms between two wells can be controlled by the population in the third similar to that of an electronic field-effect transistor. Additionally, due to similarity between multi-well system and multilevel system, the effects of nonlinear Landau–Zener tunnel and stimulated Raman adiabatic passage are also investigated theoretically by using a triple-well potential.[32,33] In our regime, not only coupling parameter between adjacent wells can be adjusted by changing the height of potential barrier, but also a controllable atomic interaction can be obtained by using extra magnetic bias field. Large separation also make it possible to address single well and control the number of atoms in each well. A tilted triple-well trap also can be obtained by varying the ratio of t_0 and t_1, which correspond to the ratio of centre well and two side wells, and the ratio of well separation and focal length corresponding the ratio of left and right one. So, our scheme can provide a robust tool for implementing such effects in experiment.

References

[1] Hoston W and You L 1996 *Phys. Rev.* A **53** 4254

[2] Andrews M R, Townsend C G, Miesner H J, Durfee D S, Kurn D M and Ketterle W 1997 *Science* **275** 637

[3] Liu W M, Wu B and Niu Q 2000 *Phys. Rev. Lett.* **84** 2294

[4] Shin Y, Saba M and Pasquini T A 2004 *Phys. Rev. Lett.* **92** 050405

[5] Wang Y J, Anderson D Z, Bright V M, Cornell E A, Diot Q and Kishimoto T 2005 *Phys. Rev. Lett.* **94** 090405

[6] Schumm T, Hofferberth S, Andersson L M, Wildermuth S, Groth S, Bar-Joseph I, Schmiedmayer J and Kruger P 2005 *Nature Physics* **1** 57

[7] Jo G B, Shin Y, Will S, Pasquini T A, Saba M, Ketterle W and Pritchard D E 2007 *Phys. Rev. Lett.* **98** 030407

[8] Jo G B, Choi J H, Christensen C A, Lee Y R, Pasquini T A, Ketterle W and Pritchard D E 2007 *Phys. Rev. Lett.* **99** 240406

[9] Ekstrom C R, Schmiedmayer J, Chapman M S, Hammond T D and Pritchard D E 1995 *Phys. Rev.* A **51** 3883

[10] Kasevich M and Chu S 1991 *Phys. Rev. Lett.* **67** 181

[11] Anderson B P and Kasevich M A 1998 *Science* **282** 1686

[12] Gupta S, Dieckmann K, Hadzibabic Z and Pritchard D E 2002 *Phys. Rev. Lett.* **89** 140401-1

[13] Shin Y, Sanner C, Jo G B, Pasquini T A, Saba M, Ketterle W and Pritchard D E 2005 *Phys. Rev.* A **72** 021604(R)

[14] Yan B, Cheng F, Ke M, Li X L, Tang J Y and Wang Y Z 2009 *Chin. Phys.* B **18** 4259

[15] Ke M, Yan B, Cheng F and Wang Y Z 2009 *Chin. Phys.* B **18** 4823

[16] Ji X M, Mu R W and Yin J P 2005 *Acta Phys. Sin.* **54** 5109 (in Chinese)
[17] Ji X M and Yin J P 2005 *J. Opt. Soc. Am.* B **22** 1737
[18] Boyer V, Godun R M, Smirne G, Cassettari D, Chandrashekar C M, Deb A B, Laczik Z J and Foot C J 2006 *Phys. Rev.* A **73** 031402(R)
[19] Fatemi F K, Bashkansky M and Dutton Z 2007 *Opt. Express* **15** 3589
[20] Melville H, Milne G F, Spalding G C, Sibbett W, Dholakia K and McGloin D 2003 *Opt. Express* **11** 3562
[21] Esslinger T, Bloch I and Hänsch T W 1998 *Phys. Rev.* A **58** R2664
[22] Seldowitz M A, Allebach J P and Sweeney D W 1987 *Appl. Opt.* **26** 2788
[23] Cataliotti F S, Burger S, Fort C, Maddaloni P, Minardi F, Trombettoni A, Smerzi A and Inguscio M 2001 *Science* **293** 843
[24] Greiner M, Mandel O, Esslinger T, Hansch T W and Bloch I 2002 *Nature* **415** 39
[25] Dalfovo F, Giorgini S, Pitaevskii L P and Stringari S 1999 *Rev. Mod. Phys.* **71** 463
[26] Adhikari S K and Muruganandam P 2003 *Phys. Rev.* A **310** 229
[27] Adhikari S K 2003 *Eur. Phys. J.* D **25** 161
[28] Dalfovo F, Giorgini S, Pitaevskii L P and Stringari S 1999 *Rev. Mod. Phys.* **71** 463
[29] Liu B, Fu L B, Yang S P and Liu J 2007 *Phys. Rev.* A **75** 033601
[30] Stickney J A, Anderson D Z and Zozulya A A 2007 *Phys. Rev.* A **75** 013608
[31] Hailei W and Shiping Y 2008 *Acta Phys. Sin.* **57** 4700 (in Chinese)
[32] Nesterenko V O, Novikov A N, de Souza Cruz F F and Lapolli E L 2009 *Laser Phys.* **19** 616
[33] Graefe E M, Korsch H J and Witthaut D 2006 *Phys. Rev.* A **73** 013617